Diffraction-limited imaging at IR wavelengths using aperture masks and fully-filled apertures

Christopher A. Haniff

California Institute of Technology, Department of Astronomy, 105-24
Pasadena, California, 91125

David F. Buscher

Mullard Radio Astronomy Observatory, Cavendish Laboratory
Madingley Road, Cambridge, CB3 OHE, UK

Julian C. Christou & Stephen T. Ridgway

National Optical Astronomy Observatories, P.O. Box 26732
Tucson, Arizona 85726-6732

ABSTRACT

The performance of a phase recovery algorithm developed for speckle data collected using a pupil-plane mask has been investigated for use at near infrared wavelengths. The method, based on the radio-astronomical self-calibration technique, has been tested alongside a state-of-the-art implementation of the Knox-Thompson scheme using both simulated and real specklegrams. Our results indicate that the new procedure is as effective as the Knox-Thompson based image reconstruction scheme and is applicable to a wide range of astrophysically interesting sources.

1. INTRODUCTION

An important development in high-resolution imaging with ground-based telescopes has been the use of non-redundant[1,2,3] and, more recently, partially redundant[4] aperture masks. As part of the ongoing speckle imaging program at the National Optical Astronomy Observatories (NOAO) we have been investigating the potential of the partially redundant mask (PRM) method at near infrared wavelengths. Fortunately in this domain the size of a typical coherence patch is sufficiently large ($\sim$ 50cm at 2μm) that the major disadvantage of the masking method, the reduction in detected flux, is not a significant concern for all but the faintest sources.

Although the conventional filled aperture speckle methods and the PRM technique differ in what may appear to be a trivial manner, there are two aspects of the PRM technique that need to be examined in detail when comparing these two methods. The first of these is the geometry of the aperture mask itself. It is well known that even in the bright source limit conventional speckle methods require that many specklegrams be collected and analyzed so as to eliminate the effects of atmospheric noise. On the other hand, the use of a non-redundant mask removes this requirement so that a single short exposure image can, in principle, be used to reconstruct the true source brightness distribution. However this advantage is tempered to some extent by a decrease in the signal-to-noise ratio (SNR) of the measurements because of the reduction in the detected photon flux. The optimum choice of a partially redundant mask thus represents a careful balance in which the competing claims of reducing atmospheric noise and maintaining a high photon rate are traded off with each other within the confines set by the seeing and the time available for the observations.

In this paper we will not address this problem, but will concentrate on the second of these issues – the algorithm used to invert the data. The scheme that we have chosen to invert our PRM data, which is modeled on the radio astronomical technique of self-calibration, is sufficiently different from currently favoured schemes employed to invert Knox-Thompson[5,6] (KT) and bispectrum[7] (BS) measurements that we felt it worthwhile to investigate its potential in some detail. Although originally conceived to reduce data from non-redundant and partially redundant mask experiments, it can be utilized to invert data obtained without a mask and so it may be of interest to a wider community. Consequently we have compared its performance with an up-to-date implementation of the KT method using conventional speckle images. Our tests, incorporating both simulations and the analysis of real data, indicate that it performs as well as the KT-based code and should thus be adopted as a valuable alternative to existing phase retrieval algorithms.

2. METHODS FOR PHASE RECOVERY

Despite the numerous advances made since the inception of speckle interferometry in the early 1970s, the fundamental problem in all diffraction-limited imaging schemes that attempt to overcome the effects of atmospheric turbulence has remained the same: the recovery of Fourier phase information. Although early experimenters attempted to perform image reconstruction from modulus only Fourier data, the interferometric schemes that have received most attention to date are able to supply the source Fourier phases directly, albeit in a "scrambled" form: either as a set of phase differences measured between closely spaced spatial frequency components, as in the KT cross spectra, or as a linear combination of the phases in the bispectrum. Thus a vital step in the image reconstruction procedure is the estimation of the true source Fourier phases from these noisy and often incomplete measurements. As an aside, we remind the reader that the phase of the bispectrum is equivalent to the so called closure phase of radio interferometry. We shall henceforth use both terms interchangeably.

2.1. Current strategies for phase recovery

Most workers have chosen to solve this inverse problem by following one of two approaches. The most popular of these takes advantage of the fact that both the KT and BS techniques provide information that has a recursive structure, in the sense that individual measurements constrain the possible values of the Fourier phase at more than one frequency. Once one or two of the phases close to the spatial frequency origin have been initialized it is possible to perform a path integral to obtain the phase at any point in the UV plane[8]. These procedures have been the subject of much study and nowadays almost always include sophisticated numerical methods that attempt to compensate for the cumulative errors that naturally arise at high spatial frequencies when recursive methods are used[9,10]. An alternative treatment, that has surprisingly received only limited attention, is to perform a global least-squares fit directly to the Knox-Thompson cross spectra or the bispectrum[11]. The limited number of pixels in current near infrared array detectors means that the cross spectral and bispectral volumes are relatively small and hence the fitting can be performed straightforwardly and rapidly using standard minimization techniques.

Both of the approaches outlined above share two features that may be expected to severly limit their potential. In almost all implementations of these methods the full cross-spectral or bispectral volumes are never employed in the inversion procedure. Instead only those near-axis regions close to the so called "seeing-ridge", which have the best SNR are utilized. However there have been a number of interesting analyses[12] which suggest that the penalty incurred by using a recursive method quickly removes the benefit that such regions apparently offer, so that it may be advisable to utilize much more of the measured Fourier data in these instances. A more important deficiency of these schemes is that they do not incorporate any *a priori* information about the source. As evidenced by their importance in schemes for image reconstruction in radio astronomy and in the complete absence of any phase information[13], constraints such as positivity and extent can be expected to offer powerful additional leverage if they can be integrated into the phase-fitting procedure itself.

2.2. An alternative formalism for phase retrieval

The method that we are advocating is based on the self-calibration[14] technique, developed in radio VLBI, and provides a means of inverting a noisy and sparsely sampled estimate of the image bispectrum to obtain the source Fourier phases. It not only makes use of the "plateau" region of the bispectrum, which potentially contains more useful information than the near axis domain, but also permits the incorporation of a wide range of extra constraints that may be appropriate to the particular source being imaged.

Self-calibration originally arose as a method of robust image reconstruction from Fourier data obtained with phase-unstable separated-element radio interferometers. In many instances the errors in the measured Fourier phases can be attributed solely to errors located at individual antennae in the interferometer. For example these may be due to differences in the paths to the source along the lines of sight from each antenna. Under these circumstances self-calibration permits the determination of the true source Fourier phases as well as the errors at each individual antenna. Although this description and the formalism involving separated elements and antenna-based errors seems far removed from the situation encountered with a single large telescope at optical and near infrared wavelengths, self-calibration can be equivalently viewed as a strategy for inverting bispectrum data to obtain source Fourier phases. This is because in a radio interferometer (or any separate-element interferometer), the closure phases are

unaffected by antenna-based phase errors and so solving for the antenna errors is equivalent to finding a set of Fourier phases that satisfy the phase-closure relations. If we take this viewpoint, then it seems only natural to consider the possibility of using existing radio astronomical self-calibration software to invert conventional speckle data. This is exactly the approach that we have chosen in this paper, using an unmodified version of the Caltech VLBI package to invert Fourier amplitude and bispectrum data extracted from conventional specklegrams.

Apart from the specific algorithms employed during the phase retrieval procedure, radio astronomical inversion schemes differ from current KT and BS schemes at a basic level because they are designed explicitly to invert sparsely sampled Fourier data. On the other hand, for the experiments reported here, the short exposure specklegrams contain information at all spatial frequencies up to the limit set by diffraction at the telescope aperture. Because of this difference, the use of radio astronomical software does require that the available Fourier data be sampled as though it had been obtained with a radio telescope array, and so it becomes impracticable to make use of all of the information in the data. However in practice this is rarely of importance as systematic effects almost always dominate before the sparseness of the UV coverage becomes noticeable.

2.2.1 Sampling the UV plane

As mentioned above, the use of VLBI software requires that the available Fourier data be sampled as if it had been obtained with a radio interferometer. A convenient strategy for accomplishing this sampling is to pick a set of N points within the telescope pupil: hereafter we shall refer to this set of locations as defining a "pseudo-array" comprising N imaginary antennae. A set of $N(N-1)/2$ baseline vectors, or spatial frequencies, can be derived from this set of N points by computing the set of all possible vectors linking pairs of these points. Similarly a set of $N(N-1)(N-2)/6$ bispectrum coordinates can be computed by enumerating all possible loops joining triplets of these points and identifying the relevant spatial frequencies with each leg of these triangles. Since the number and locations of these imaginary antennae are free parameters in this scheme, it is possible to generate a large number of different "combs" with which to sample the available Fourier data. However the most useful pseudo-arrays will be those that sample the UV plane as completely and uniformly as possible. A review of the numerical methods employed to optimize the pseudo-array configuration is beyond the scope of this paper[15], but we note that excellent sampling can be achieved with as few as 15 antennae. An example of such a pseudo-array and its UV coverage is shown in figure 1.

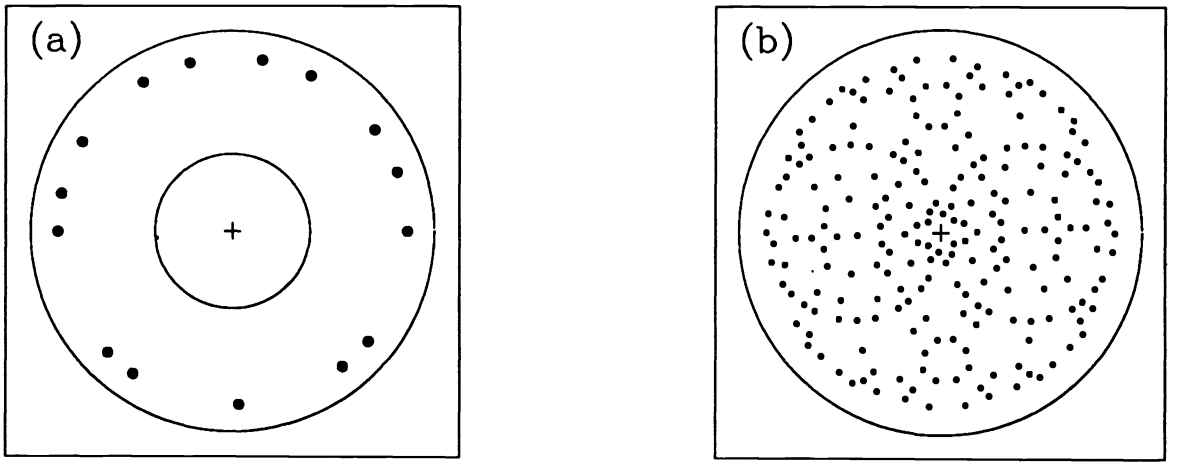

Figure 1. Antenna positions (a) and UV coverage (b) for a 15 element pseudo-array. Circles plotted in each figure show the boundaries of the telescope pupil and its transfer function respectively. Note that even with as small a number of elements as 15, the UV coverage is quasi-uniform and relatively complete.

2.2.2 Data reduction

In the course of an actual experiment the choice of a pseudo-array usually takes place before any of the data is reduced, and the power spectrum and bispectrum are subsequently accumulated only at the coordinates appropriate

to the particular array. This allows a modest reduction in the computation required for our scheme when compared to most KT and BS based methods, which may be important if computer resources are at a premium. The mean power spectrum and bispectrum values are then calibrated in the usual manner using data obtained on an unresolved source.

Most radio astronomical self-calibration software packages expect data in the form of visibility amplitude and phase measurements for each baseline, although it is implicitly accepted that there are arbitrary antenna-based errors in the phase measurements. This format is slightly inconvenient for data from optical and near infrared interferometry, because the Fourier phase measurements can only be averaged in the form of the bispectrum, and these data must then to be mapped back into the space of baseline phases. However, it must be remembered that the problem here is only to find a set of phases that are consistent with the bispectrum phases - the self-calibration software will find that particular set which satisfies the *a priori* constraints and the phase closure relations simultaneously. The selection of a suitable set of Fourier phases can be performed in many ways, for example using the generalized inverse of Lannes[16], but we have chosen to obtain them by fitting directly to the measured bispectrum phases in a least-squares sense using a simple conjugate-gradient method. This method has the advantage that it permits a proper treatment of the measurement errors to be included during the backprojection.

In summary, by sampling the Fourier plane as explained above, and selecting a set of Fourier phases that are consistent with the measured bispectrum phases, we can prepare a dataset that corresponds in all respects to that which would have been observed with an N element radio interferometer under phase unstable conditions. In order to minimize any confusion, we stress once more that the notional antenna-based phase errors associated with the N elements of the pseudo-array bear no relation to the actual atmospheric fluctuations present while the interferograms were recorded. They merely provide a useful framework in which the case for using radio astronomical software can be seen most clearly, and in which the basis for bispectral imaging and its relation to the closure phase are elegantly revealed.

2.3 Self-calibration

Once a sampled dataset, comprising visibility amplitudes and corrupted phases, has been prepared it can be inverted using any standard radio astronomical self-calibration package. Since the rationale and software implementation of self-calibration has been described in the literature many times[17,18] we refer the reader to these references, and will simply restate that it provides a robust strategy for estimating the N antennae-based errors that are assumed to have corrupted the measured Fourier data, thereby simultaneously solving for the unperturbed source Fourier phases. Most importantly the solution is reached in an iterative and model-independent manner in which many types of *a priori* information about the source can be included if required. Examples of such information might be knowledge of the maximum source extent, its non-negativity or an initial estimate of its morphology based on a low resolution image. For the self-calibration reconstructions presented here we have not used any extent or positivity constraints explicitly, but have taken advantage of the implicit assumptions of the CLEAN[19] algorithm which forms part of the iterative phase estimation loop of the Caltech implementation of self-cal.

3. NUMERICAL SIMULATIONS

In order to compare our proposed data reduction scheme with existing methodologies in a controlled manner, we have inverted a number of sets of simulated near-infrared specklegrams using our new scheme and with the latest version of the NOAO Knox-Thompson code. The major details of the NOAO code have been described before[20] so we simply present a flow chart outlining the steps in the latest version of the code in figure 2. A similar flow diagram for the steps in our self-calibration based algorithm is shown in figure 3. The pseudo-array used for these tests comprised 17 elements, giving a total of 136 UV points and 680 bispectrum points.

For simplicity, we chose to explore a small region of the possible parameter space corresponding to observations made with a 4-metre class telescope under average seeing conditions. In addition we restricted our attention to moderately bright sources. Four test objects were selected, comprising a rather wide binary star with separation 0.48″ and flux ratio 0.85, a close binary with separation 0.20″ and flux ratio 0.10, together with two sources of more complex morphology. The first of these complex sources was rather compact and only partially resolved at the cut-off frequency of the telescope, whereas the second was composed of several superposed components and was

considerably more extended, though of course smaller than the seeing limit. Contour plots of these 4 sources, at a resolution appropriate to a diffraction-limited 4-metre telescope, are displayed in figures 4a, 4d, 4g and 4j.

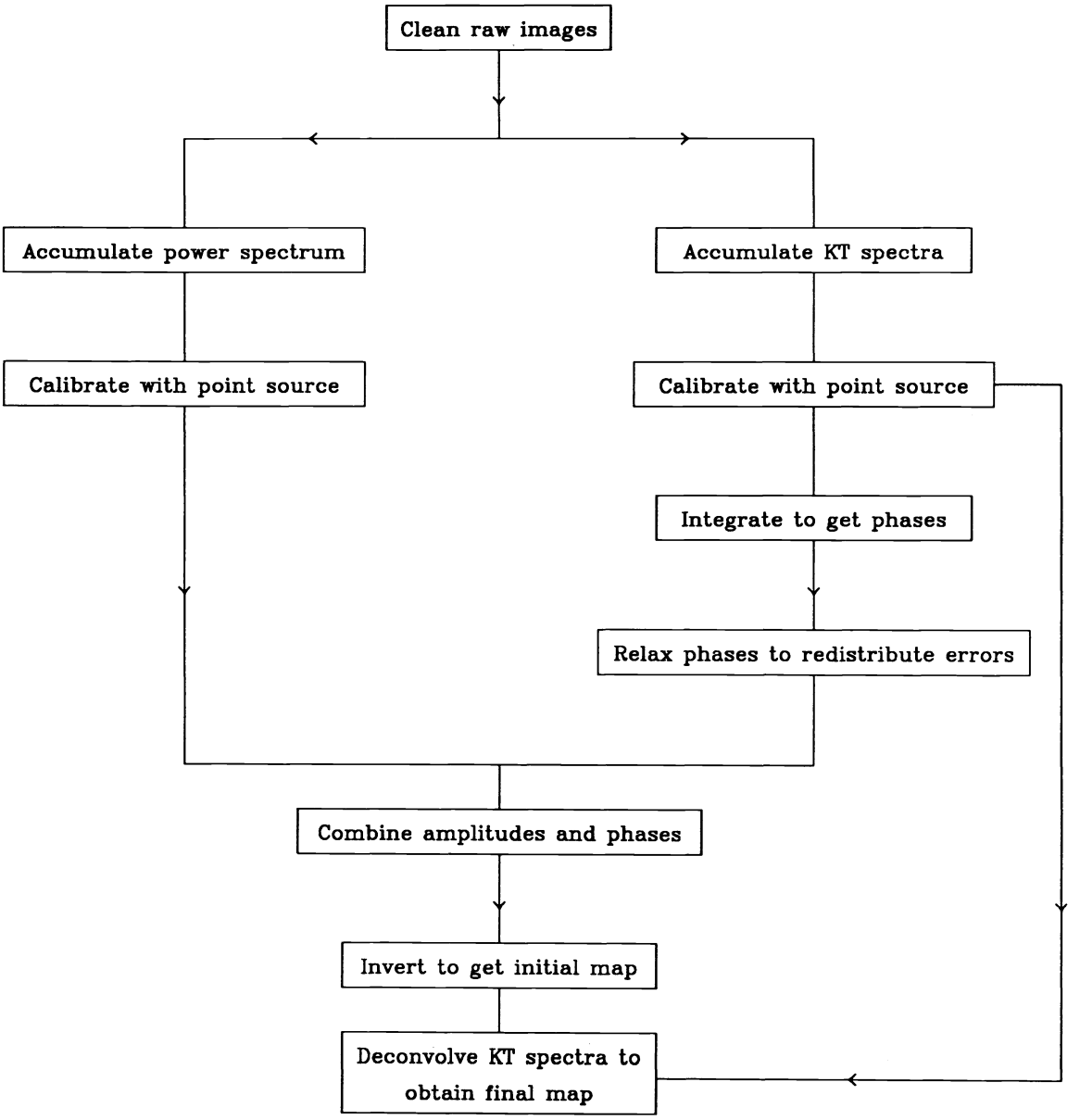

Figure 2. Flow diagram outlining the basic steps in the Knox-Thompson inversion scheme employed for this paper. In this version of the KT algorithm, the source Fourier phases are initially solved for without including any *a priori* information about the object, and subsequently "corrected" in the final iterative-deconvolution[21] loop where positivity and extent constraints can be applied.

500 independent speckle interferograms were prepared for each of these test objects, together with 1000 separate interferograms of an unresolved calibration source. The interferograms corresponded to short exposure integrations taken with a 3.8 metre telescope in 1″ seeing, as measured at 5000Å. The images were corrupted with Gaussian zero-mean noise, to mimic the effects of the detector readout noise, but did not incorporate any noise due to either photon statistics or thermal background emission, both of which are negligible for the source parameters we have chosen. In addition the finite exposure time and spectral bandwidth were assumed to be sufficiently small that

atmospheric decorrelation could be neglected, an assumption that is almost always likely to be satisfied in the near infrared. Scaling the readout noise to a typical value of ~ 450 electrons per pixel, we calculate that the effective K magnitudes of the test sources were 5.6 for the binary and calibration stars and 4.6 and 4.3 for the two extended sources respectively. As a final test we have also attempted to assess the reliability of each reconstruction scheme by preparing another set of speckle images of the most extended source, identical in all respects to the original set but with twice the readout noise, corresponding to an effective K magnitude of 5.0.

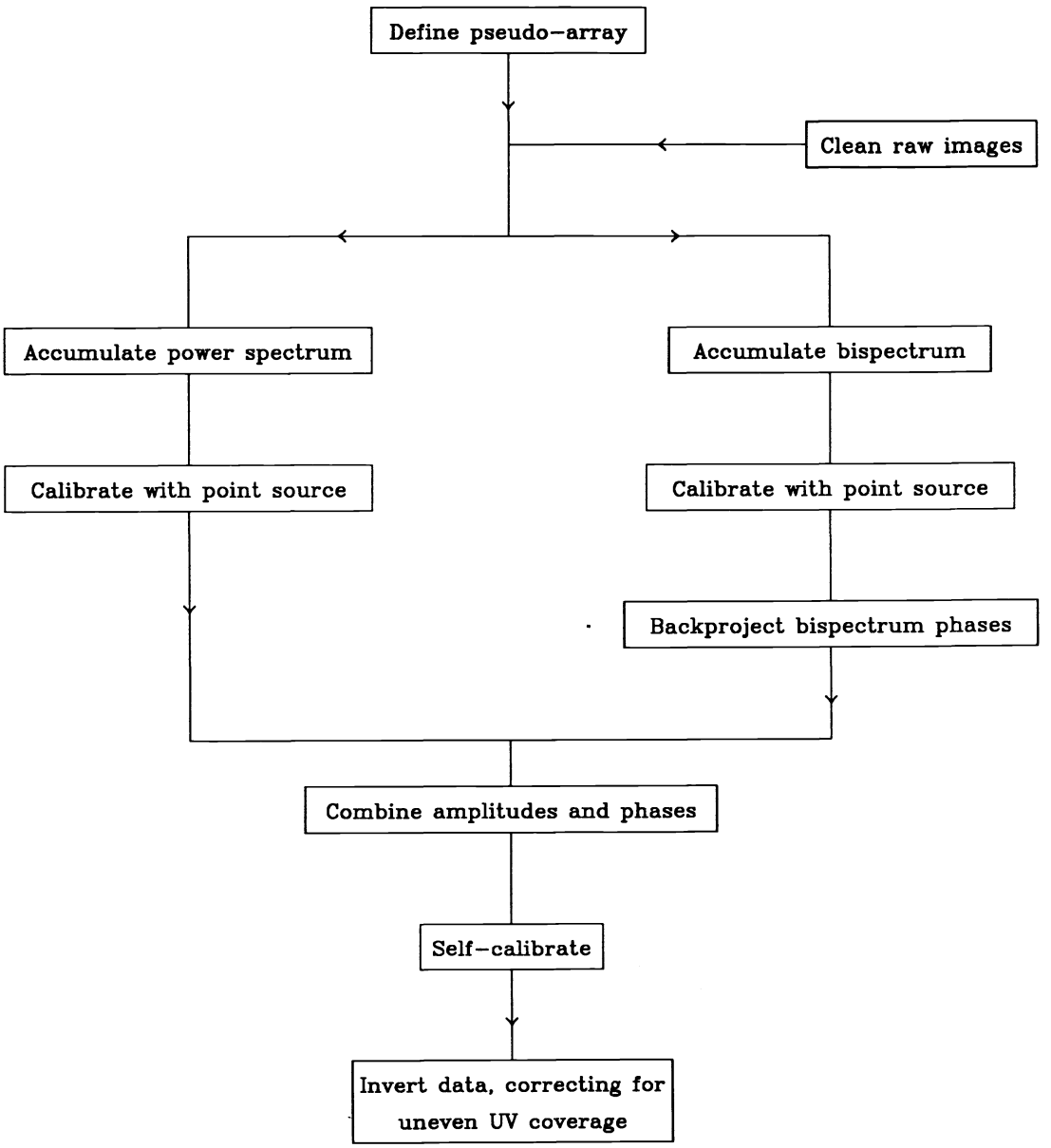

Figure 3. Flow diagram outlining the basic steps in the self-calibration based inversion scheme employed for this paper. The bispectrum and power spectrum are only accumulated at the coordinates defined by the pseudo-array. Note that the radio astronomical based steps have been split into two parts: an initial stage where the antenna based errors are estimated, denoted by the box marked "self-calibration", and a final step where the corrected Fourier data are inverted and the resulting map is deconvolved to compensate for the sparse UV coverage of the pseudo-array.

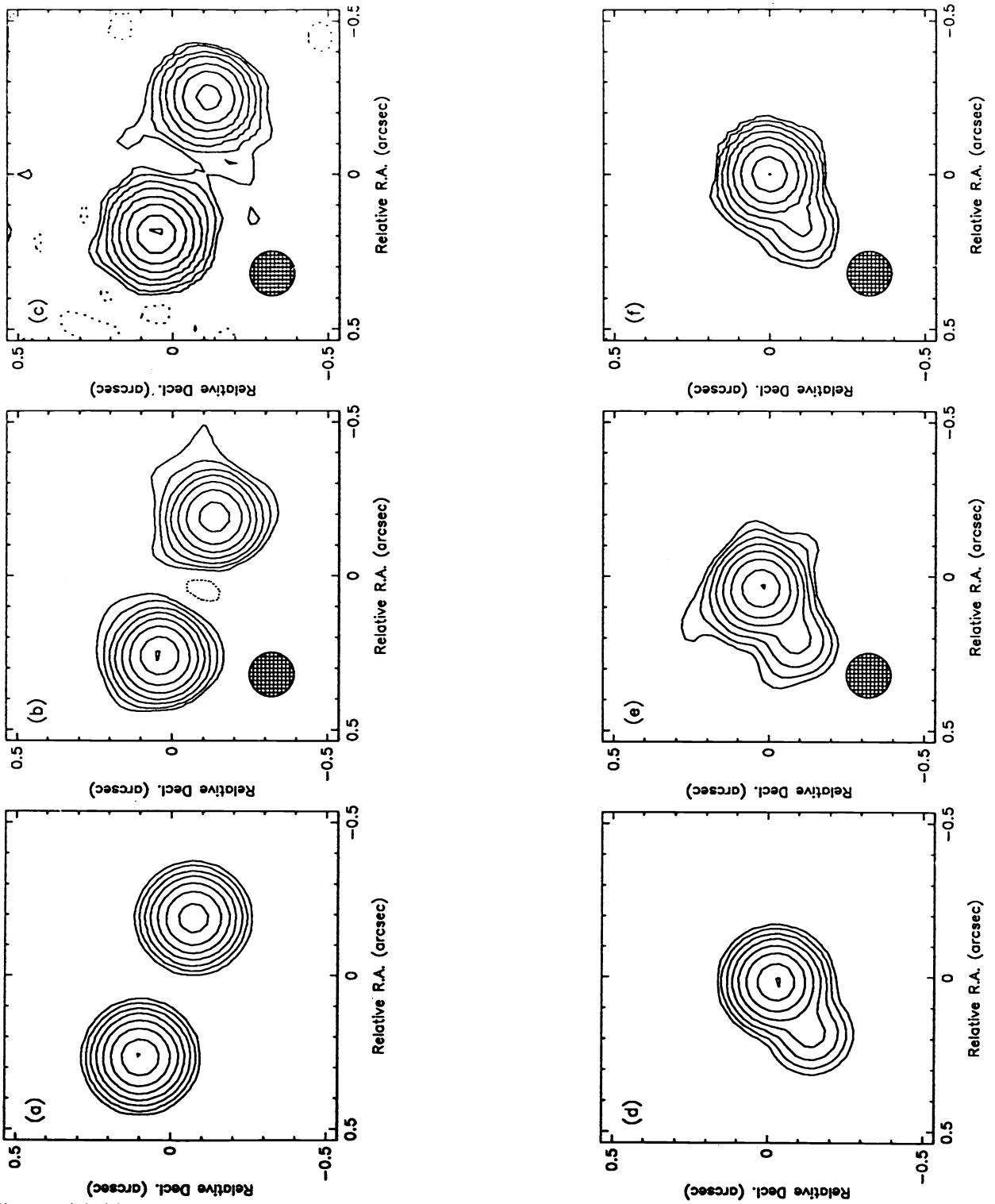

Figure 4(a)-(f). Image reconstructions of the 2 binary star test sources used to compare the Knox-Thompson and self-calibration inversion strategies. Each horizontal sequence shows a diffraction limited image of the test source and then the KT and self-calibrated maps derived from 512 simulated specklegrams. All the maps are contoured at identical levels of -2, -1, 1, 2, 4, 8, 16, 32, 64 and 99% of the peak intensity and have the same resolution, which is represented by the hatched circle in the lower left hand corner of each panel.

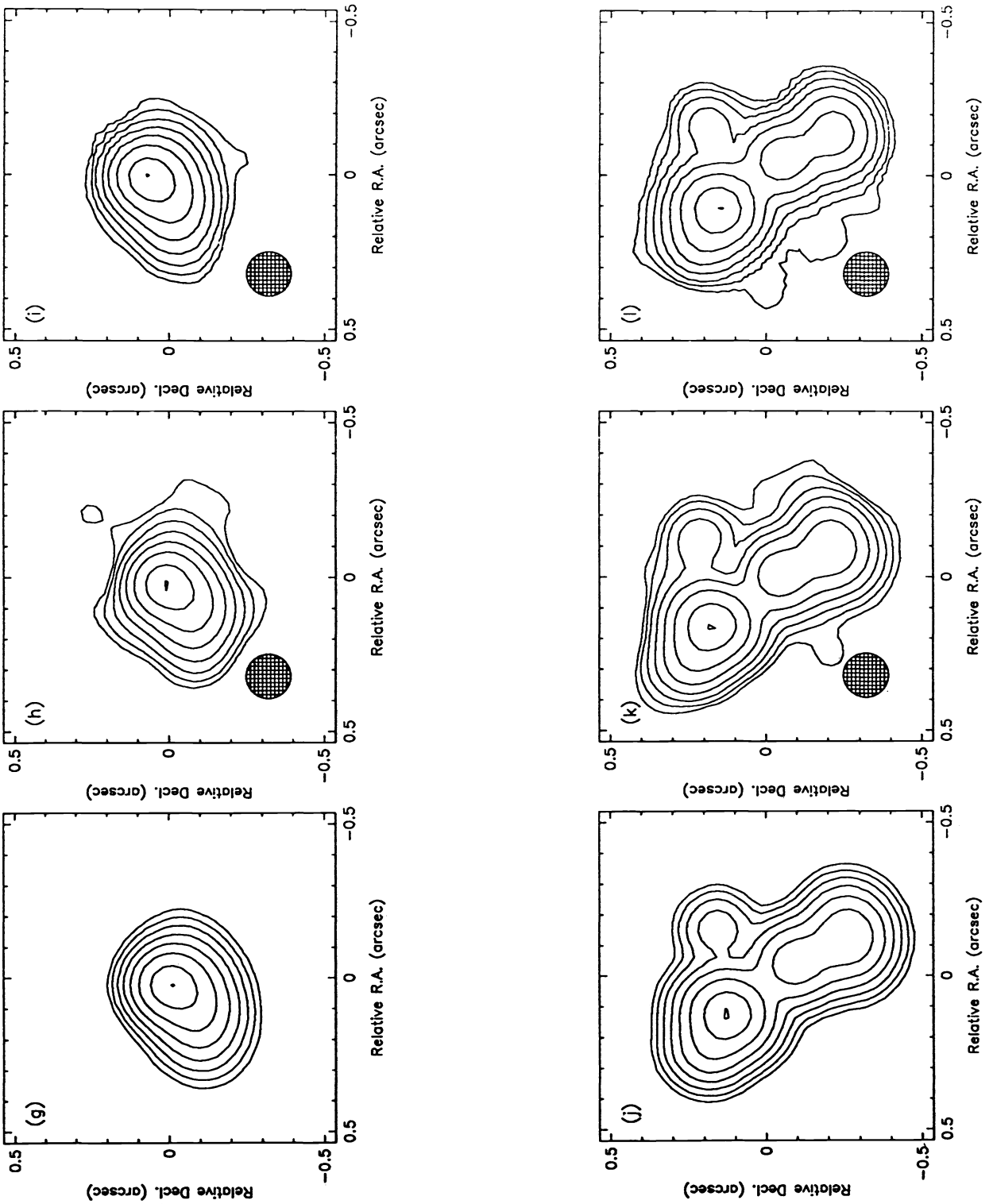

Figure 4(g)-(l). KT and self-calibrated image reconstructions of the 2 extended test sources obtained from 512 simulated interferograms. The sequence in each panel, contour levels and resolution are identical to those in figures 4(a)-(f).

3.1 Binary star reconstructions

The KT and self-calibrated reductions of the wider of the 2 binary stars are shown in figures 4b and 4c. In these and all subsequent plots the contour levels are drawn at -2, -1, 1, 2, 4, 8, 16, 32, 64 and 99% of the peak flux in the map. The quality of both images is very good, with spurious noise features only becoming apparent at a level of 1% of the peak intensity, where the individual components of the system become non-circular. Although this is a rather wide binary, the approximate equality of the component fluxes ensures that the visibility function drops towards zero frequently and so this is a relatively difficult object to image accurately. Nevertheless the separate reconstructions give almost identical values for the component fluxes, separations and position angles, which agree very well with the model source parameters.

The image reconstructions of the closer binary, figures 4e and 4f, are once again similar, although the KT reconstruction begins to show spurious extensions at the 1% flux level. These are not seen in the self-calibrated image which shows no noise features at all at this level and has a dynamic range of approximately 150:1. As expected both maps, which have identical resolutions, are unable to split the component stars completely, but the flux, position angle and separation of the secondary component are well determined in both cases.

3.2 Extended source reconstructions

The first extended test source is only barely resolved at the diffraction limit of the simulations and so the quality of the image reconstructions is similar to that of the closer of the two binary stars. Once again the self-calibrated image, figure 4i, is marginally superior than the KT image, figure 4h, which begins to show ragged contours at the 1% level. Neither map shows any other noise features at the lowest contour level plotted, and both reveal the extended nature of the source clearly, including the gentle curve of the major lobe towards the east.

The second of the extended test sources presents the most difficult challenge to either inversion method because it is heavily resolved at many spatial frequencies and extends over many beamwidths. Not surprisingly the contour level at 1% of the peak intensity shows spurious excursions in both maps (figures 4k and 4l). Otherwise the separate inversions are in all significant respects identical and closely resemble the image expected in the absence of turbulence. The final dynamic range achieved in these reconstructions is approximately 75:1.

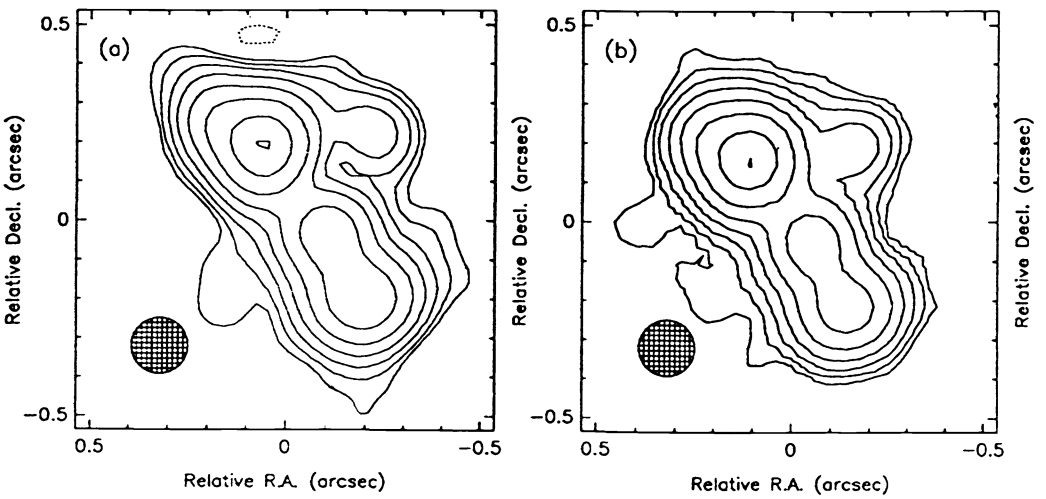

Figure 5. Low SNR Knox-Thompson (a) and self-calibrated (b) image reconstructions of the second extended test source (figure 4j). These are to be compared with figures 4k and 4l which were obtained from data with twice the SNR. The contour levels plotted are identical to those in the previous figure.

To investigate the behaviour of each algorithm with noisier data, a final test was performed using identical speckle realizations of the most extended source but corrupted with twice the zero-mean Gaussian noise. The KT and self-calibrated reconstructions from this noisier ensemble are shown in figures 5a and 5b where they are contoured

at the same levels used in figure 4. The KT image shows a distinct deterioration in the presence of this extra noise, but somewhat surprisingly, the self-calibrated image is only marginally different at the lowest contour level. This suggests that in this regime the reliability of the self-calibrated image is limited by the residual atmospheric noise in the visibility data, but that this may not be the case for the KT inversion.

4. TESTS WITH REAL DATA

Although numerical simulations can provide some insight into the merits of the two inversion strategies under study here, experience suggests that the systematic, and unexpected, problems that often occur during actual observations provide a far more valuable testing ground for any worthwhile speckle imaging scheme. Consequently we have attempted to invert two separate near infrared speckle datasets; the first for the binary star η Ophiuchi and the second for the evolved supergiant star IRC 10216.

Speckle images of these objects were obtained on the nights of the 21-22 May 1989 at the Cassegrain focus of the Mayall 3.8m telescope at Kitt Peak National Observatories. The images were recorded with the NOAO speckle camera[22], using an integration time of 50ms per exposure and a 0.09μm filter centred on 2.22μm. Long exposure images of the calibration sources used for these data had full widths at half-maximum intensity of $\sim 1.0''$.

The KT and self-calibrated reconstructions derived from 1024 specklegrams of η Ophiuchi are shown in figures 6a and 6b. Although this source has a K magnitude of 2.4 these images are of substantially lower quality than the simulated reconstructions displayed in figure 4. Both images show curving tails of weak emission extending to the north east and south west of the binary components together with several blobs of noise emission spread over the field of view. The curved wings limit the dynamic range of these maps to approximately 25:1 which is well below that expected on the basis of our numerical simulations. However the fact that both image reconstructions show similar artifacts suggests that systematic effects are responsible for the poor quality of these maps. Probable causes include residual atmospheric noise or alternatively a bad seeing mismatch between the source and calibrator observations. Although both of the algorithms appear to be susceptible to such problems, it is reassuring to see that they behave similarly and resolve this binary with ease.

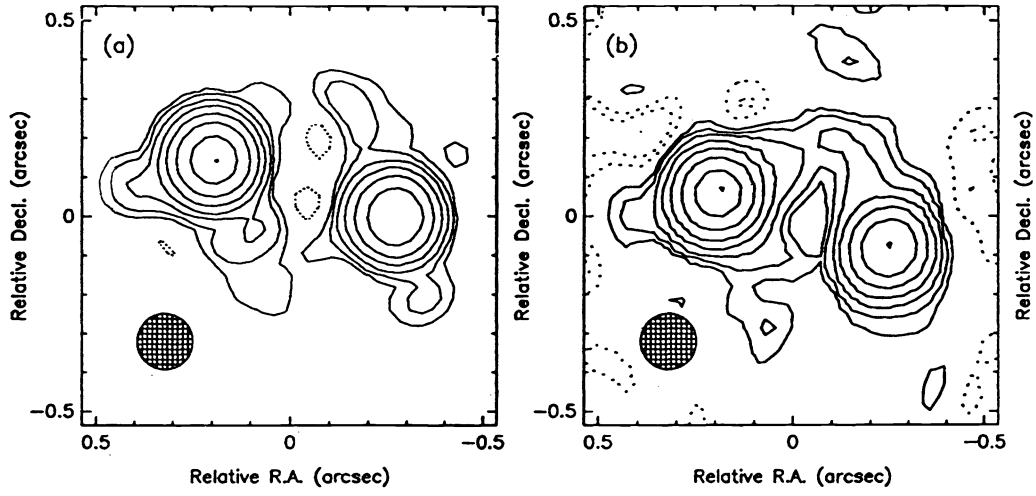

Figure 6. Knox-Thompson (a) and self-calibrated (b) image reconstructions of the close binary star η Ophiuchi. The contour levels are at -2, -1, 1, 2, 4, 8, 16, 32, 64 and 99% of the peak intensity. North is to the top and east to the left. A 17 element pseudo-array was used for the self-calibrated reconstruction.

Figures 7a and 7b show the KT and self-calibrated images of IRC 10216, obtained from 1536 specklegrams, contoured at the same levels as figure 6. Both maps show a resolved core with extensions to the northeast and southwest. In the KT image the northern extension is more prominent and the southern feature is most clearly seen as an elongation of the higher contour levels. There is also evidence for a diffuse halo of emission towards the north and east, but the lowest contour level is probably not reliable as evidenced by the negative feature to the southwest of

the core. The self-calibrated image is similar, showing fingers of emission to the northeast and southeast, but there is no evidence of any diffuse component down to 1% of the peak flux, where the map becomes unreliable. However observations taken on other nights suggest that the weak extended component in the KT image may be an artifact due to rapid variations in the seeing while these data were being collected. In addition the self-calibrated image appears to indicate that the northern and southern extensions are of almost equal magnitude. Nevertheless the overall qualitative agreement between the two images is good, demonstrating that both methods are able to recover much of the intriguing source structure lost in a long exposure image.

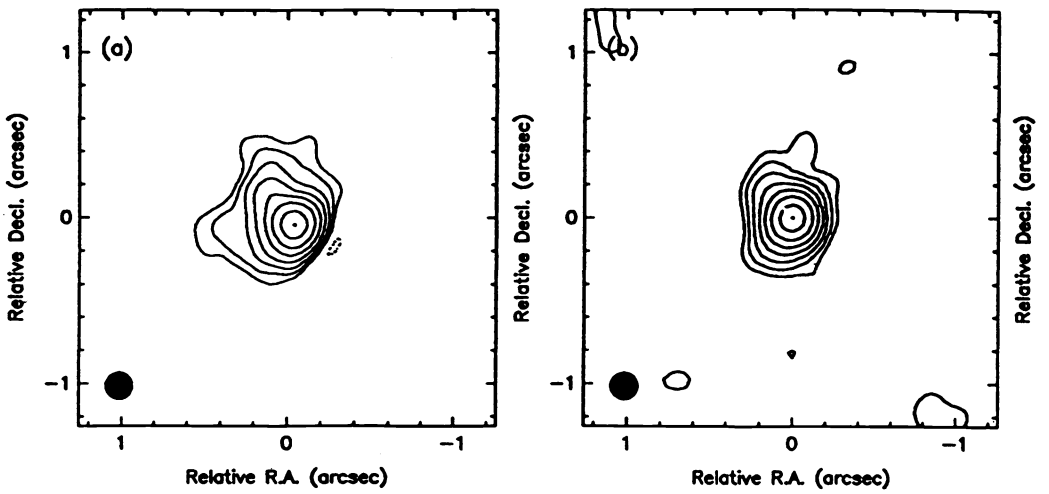

Figure 7. Knox-Thompson (a) and self-calibrated (b) image reconstructions of the evolved carbon star IRC 10216. The contour levels and orientation are the same as figure 6. These images reveal for the first time the peculiar bi-lobed structure that has been previously hinted at by one-dimensional speckle observations. Note that only a 12 element pseudo-array has been used for the self-calibrated reconstruction.

5. DISCUSSION

The most striking result of the maps presented in the previous sections relates to the quality of the self-calibrated image reconstructions. In all cases they have a similar or marginally better dynamic range than their KT counterparts despite the fact that have been recovered from only a small fraction of the available Fourier data. The particular 17 element pseudo-array employed for most of these tests samples approximately 10% of the UV plane, and a correspondingly smaller proportion of the bispectral space, yet the recovered images do not appear to have been compromised in any way by the sparseness of the UV and bispectral coverage. With real data, both techniques appear to produce images that are limited by systematic effects rather than the particular inversion method employed.

This suggests, as do the images obtained from the lowest signal-to-noise ratio simulations, that the quality of these images is determined primarily by the residual atmospheric noise and not by the Fourier plane coverage. There is also tentative evidence that the self-calibration scheme is more robust in the presence of noise. The most plausible explanation for the performance of the self-calibration scheme is that it manages to integrate extra *a priori* information about the source during the the inversion of the bispectral data. It is interesting to note that the KT reconstructions become far inferior to the self-calibrated images if the final iterative deconvolution of the cross spectrum is not performed. Since this is the only stage in the KT-based scheme in which the positivity and extent of the image are examined, this is additional evidence that these features provide the most valuable constraints in the phase recovery procedure. In the Caltech VLBI package employed for these inversions, these constraints are implicitly incorporated during the CLEANing of the dirty-maps where the interpolation between the measured visibility points is performed. This effect is rather subtle and takes place whether or not the CLEANing is restricted to certain "windows" or whether negative CLEAN components are rejected. Alternatively if a maximum entropy method is used to perform the deconvolution instead, an appropriate choice of "default map" can be used to explicitly embody a wide range of possible image constraints.

Apart from the obvious success of the phase recovery step, another benefit of our inversion scheme is that it is

extremely cheap in terms of computing resources. The fraction of CPU time spent inverting the Fourier data, is typically less than 5% of the total time required to accumulate and calibrate the raw visibility and bispectrum measurements, which is itself dominated by the single Fast Fourier Transform performed on each specklegram. Arguably the most valuable feature of the self-calibration scheme though is the fact that it is a mature and well tested technique. In particular its undesirable aspects and intrinsic biases, when dealing with certain types of data, have been explored at length by radio astronomers so that it is relatively straightforward to identify, and then trace the causes of, any artifacts in the reconstructed image should they occur.

Since we originally proposed the self-calibration strategy for reducing speckle data recorded with a pupil plane mask, our scheme does not require that the telescope pupil be filled. Consequently, should the use of an apodized pupil be advantageous[23], which may be the case if the source is sufficiently bright, there will be no deterioration in its efficiency. In addition, the selection of a discrete number of coordinates in the UV plane allows the user to reject spatial frequencies that may have been corrupted due to detector effects. However despite this useful flexibility and the success of these tests, it is evident that our scheme falls short in a number of respects. Most noticeable is the need to discard a large proportion of the Fourier information in the specklegrams. Although this does not appear to have been a limiting factor in any of the reconstructions presented here, higher dynamic range mapping will inevitable require better UV coverage. An associated problem is that it is difficult to design pseudo-arrays that exploit the highest SNR bispectral data, located along the seeing ridge, while maintaining quasi-uniform UV coverage. We are currently investigating possible hybrid schemes that encompass the best features of the filled aperture and self-calibration methods in the hope of arriving at an optimal algorithm.

6. CONCLUSIONS

Tests using both real and simulated near infrared speckle data have been undertaken to examine the performance of a novel bispectral inversion scheme. This method, based on radio astronomical self-calibration techniques, was originally conceived to invert data obtained with non and partially redundant masks. Nevertheless when applied to conventional filled aperture speckle data it appears to be as effective as the most up-to-date versions of the Knox-Thompson scheme, even in the absence of up to 90% of the available Fourier information. These results suggest that existing methods for phase recovery from cross or bi-spectra are not as effective as they might be, and can be enhanced significantly by combining as much *a priori* information about the source with the measured data while retrieving the Fourier phase. Unfortunately, image reconstructions obtained from real data confirm that systematic effects, such as seeing variations and detector imperfections, may represent a significant barrier to progress if very high dynamic range mapping is required.

7. ACKNOWLEDGMENTS

Partial funding for this research was provided by the SERC, Christ's College Cambridge and Royal Commission for the Exhibition of 1851. CAH would like to thank Tim Cornwell and Andrea Ghez for helpful discussions while this manuscript was being prepared. The National Optical Astronomy Observatories are operated by the Association of Universities for Research in Astronomy, Inc., under cooperative agreement with the National Science Foundation.

8. REFERENCES

1. W.T.Rhodes, J.W.Goodman, "Interferometric technique for recording and restoring images degraded by unknown aberrations," *J. Opt. Soc. Am.*, Vol 63, pp. 647-657, 1973
2. C.A.Haniff, C.D.Mackay, D.J.Titterington, D.Sivia, J.E.Baldwin, P.J.Warner, "The first images from optical aperture synthesis," *Nature*, Vol 328, pp. 694-696, 1987
3. A.C.S.Readhead, T.Nakajima, T.J.Pearson, G.X.Neugebauer, J.B.Oke, W.L.W.Sargent, "Diffraction-limited imaging with ground-based optical telescopes," *Astron. J.*, Vol 95, pp. 1278-1296, 1988
4. C.A.Haniff, D.F.Buscher, J.C.Christou, S.T.Ridgway, "Synthetic aperture imaging at infrared wavelengths," *Mon. Not. R. astr. Soc.*, Vol 241, pp. 51p-56p, 1989
5. K.T.Knox, B.J.Thompson, "Recovery of images from atmospherically degraded short-exposure photographs," *Astrophys. J.*, Vol 193, pp. L45-L48, 1974
6. K.T.Knox, "Image retrieval from astronomical speckle patterns," *J. Opt. Soc Am.*, Vol 66, pp. 1236-1239, 1976
7. A.W.Lohmann, G.Weigelt, B.Wirnitzer, "Speckle masking in astronomy: triple correlation theory and applications," *Appl. Optics*, Vol 22, pp. 4028-4037, 1983

8. H.Bartelt, A.W.Lohmann, B.Wirnitzer, "Phase and amplitude recovery from bispectra," *Appl. Optics,* Vol 23, pp. 3121-3129, 1984
9. S.M.Ebstein, "Speckle imaging of active galactic nuclei NGC 1068 and NGC 4151," *Ph.D. Thesis,* Harvard University, 1988
10. O.von der Lühe, "Application of the Knox-Thompson method to solar observations," *Proc. ESO-NOAO joint workshop on "High angular resolution from the ground using interferometric techniques",* NOAO, Ed. J.Goad, pp. 37-41, Oracle, 1987
11. P.W.Gorham, A.M.Ghez, S.R.Kulkarni, T.Nakajima, G.Neugebauer, J.B.Oke, T.A.Prince, "Diffraction-limited imaging. III. 30mas closure phase imaging of six binary stars with the Hale 5m telescope," *Astron. J.,* Vol 98, pp. 1783-1799, 1989
12. D.F.Buscher, "Aperture masking and speckle masking: a comparison of their signal-to-noise ratios," *Proc. ESO-NOAO conference on "High-resolution imaging by interferometry",* Ed. F.Merkle, pp. 613-626, Garching, 1988
13. J.R.Fienup, "Phase retrieval algorithms - a comparison" *Appl. Optics,* Vol 21, pp. 2758-2769, 1982
14. T.J.Cornwell, P.J.Wilkinson, "A new method for making maps with unstable radio interferometers," *Mon. Not. R. astr. Soc.,* Vol 196, pp. 1067-1086, 1981
15. T.J.Cornwell, "A novel principle for the optimization of the instantaneous Fourier plane coverage of correlation arrays," *IEEE Trans. Antennas Propagat.,* Vol AP-36, pp. 1165-1167 1988
16. A.Lannes, "Backprojection mechanisms in phase-closure imaging. Bispectral analysis of the phase-restoration process," *Experimental Astronomy,* Vol 1, pp. 47-76, 1989
17. T.J.Pearson, A.C.S.Readhead, "Image formation by self-calibration in radio astronomy," *Ann. Rev. Astron. Astrophys.,* Vol 22, pp. 197-130, 1984
18. T.J.Cornwell, E.B.Fomalont, "Self-calibration," *Astronomical Society of the Pacific conference series: "Synthesis imaging in radio astronomy",* Eds. R.A.Perley, F.R.Schwab, A.H.Bridle, Vol 6, pp. 185-197, 1989
19. J.A.Högbom, "Aperture synthesis with a non-regular distribution of interferometer baselines," *Astron. Astrophys. Suppl.,* Vol 15, pp. 417-426, 1974
20. J.C.Christou, J.M.Beckers, J.D.Freeman, S.T.Ridgway, R.G.Probst, "Two-dimensional infrared astronomical speckle interferometry," *Proc. SPIE conference on "Statistical Optics",* Ed. G.M.Morris, Vol 976, pp. 193-203, San Diego, 1988
21. G.R.Ayers, "Deconvolution of spatial-correlation spectra for high-resolution astronomical imaging," *Optics Letters,* Vol 14, pp. 1165-1167, 1989
22. J.M.Beckers, J.C.Christou, R.G.Probst, S.T.Ridgway, O.von der Lühe, "First results with the NOAO 2-D speckle camera for infrared wavelengths," *Proc. ESO-NOAO conference on "High-resolution imaging by interferometry",* Ed. F.Merkle, pp. 393-400, Garching, 1988
23. G.R.Ayers, "Effect of pupil plane masking on the signal-to-noise ratio of atmospheric transfer functions," *These proceedings.*